

# Planning and Control for THBIP-I Humanoid Robot

Chenglong FU<sup>1</sup>, Mei SHUAI<sup>2</sup>, Kai XU<sup>1</sup>, Jiandong ZHAO<sup>1</sup>, Jianmei WANG<sup>1</sup>, Yuanlin HUANG<sup>1</sup>, and Ken CHEN<sup>1</sup>

<sup>1</sup>Department of Precise Instrument and Mechanology, Tsinghua University

<sup>2</sup>Department of Mechatronics Engineering, Beihang University

Beijing, P. R. China

kenchen@mail.tsinghua.edu.cn

**Abstract** — This paper presents the gait planning method and control strategy for THBIP-I (Tsinghua Biped Humanoid Robot) to realize stable walking. This robot includes a head, a trunk, two arms, two legs, and two feet, totally 32 DOF (degree of freedom). This project is involved for five years and aimed to realize stable walking in various environments for a self-contained humanoid robot. Firstly, the design issues including mechanical structure and control architecture of the robot are prescribed. Secondly, gait generation method based on optimization of the main support leg is presented, and control strategy composed of local joint controller and sensory feedback controller is also illustrated. The walking experiments show that the robot has the abilities of stable walking on the ground, turning in any direction, and climbing up/down stairs.

**Index Terms** – gait planning; control strategy; joint controller; sensory feedback; humanoid robot.

## I. INTRODUCTION

Humanoid robots are expected to take an important role in assisting human activities in human daily environments because of its flexibility and friendly appearance. To realize this goal, the stable biped walking in various environments is one of the most fundamental requirements. The inherent instability of a biped robot is the fundamental problem that creates this challenge. Unlike multi-legged robots that can benefit from a stable base of three and more contact regions, a biped robot has to maintain its stability with only one or two contact regions.

There are a number of humanoid robots that have been built by various groups throughout the world recently. Researchers at Waseda University enjoy a long history of working on biped robots since 1966, and they recently developed a biped humanoid robot – WABIAN-2. This robot has 41 DOF totally and can perform stretch walking patterns with straight legs which are effective in terms of energy consumption [1]. After ten years of secret research, Honda Corporation developed the humanoid robot P2, P3, and Asimo, which can perform several complicated tasks such as walking on a flat ground, turning, up/down stairs, balance, and running. The control method of Honda's robot is using ZMP to plan the pre-recorded joint trajectories and play them back with sensor-based compliant control [2]. University of Tokyo constructed humanoid robot H6 and H7 [3]. The two robots can walk up

---

This work was supported by Tsinghua University "985" Humanoid Project and the National Natural Science Foundation of China (NSFC), under grant: 50575119.

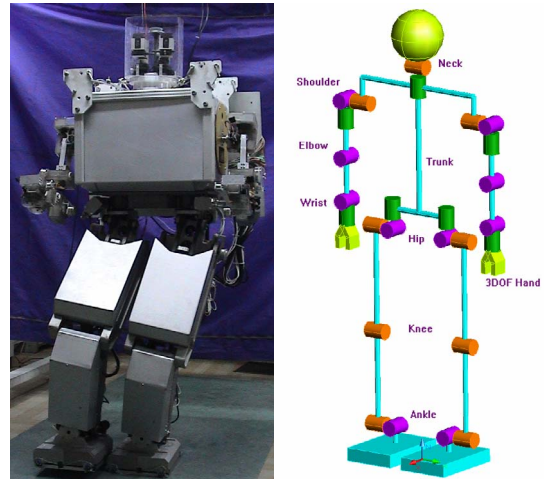


Fig. 1 THBIP-I humanoid robot and its DOF configuration

and down 25 [cm] high steps and can also recognize pre-entered human faces. Technical University of Munich constructed an anthropomorphic autonomous biped robot JOHNNIE for realization of dynamic 3-D walking and jogging motion [4]. JOHNNIE with 17 DOF is about 1800 [mm] height and about 40 [kg] weight respectively, while the operating power is supplied by external sources. Sony Corporation also developed several compact size humanoid robots including SDR-3X, SDR-4X [5], and QRIO. These robots can more than just walk around such as squatting, getting up, and running. The Ministry of Economy, Trade and Industry (METI) of Japan had run Humanoid Robotics Project (HRP) from 1998 to 2002. The final goal of HRP is to create 'useful' humanoid robots. Towards the goal, HRP have developed a humanoid robot called HRP-2 that can walk, lie down and get up [6]. Recently, Beijing Institute of Technology has developed a humanoid robot BHR-02, and this robot can perform some complicated dynamic motion, such as Chinese "sword" Kungfu, based on human motion capture [7].

For research and development of humanoid robot performing application tasks, Tsinghua University is developing a humanoid robot called THBIP-I (Tsinghua Biped Humanoid Robot), which is supported by the Tsinghua University 985 Humanoid Biped Project [8], [9]. One goal of this project is to realize a complete online motion control of the biped robot walking in various environments based on a sensory feedback control. Presently this robot has the abilities of stable walking on the ground, turning in any direction, and climbing up/down stairs continuously.

This paper presents the gait planning method and control strategy for THBIP-I. The rest of this paper is organized as follows. Section II introduces the design issues including mechanical design and control architecture of the robot. Section III presents a gait generation method based on optimization of the main support leg. Section IV introduces the control strategy to realize stable walking. Section V introduces the walking experiments, and Section VI concludes the paper.

## II. THE 32-DOF HUMANOID ROBOT

### A. Mechanical Structure

THBIP-I is a self-contained humanoid robot with two arms and two legs, and can be operated via wireless communication. Its lower limbs have 12 degrees of freedom (DOF) in two legs, which provides the robot with the abilities of walking on the ground, turning in any direction, and climbing up/down stairs continuously. Its upper limbs have 16 DOF, and its hand is similar to a two-fingered gripper with 2 DOF. It is able to open and close between its thumb and the other fingers, which forms a single moveable digit.

Fig.1 shows the figure of THBIP-I humanoid robot and the DOF configuration of the robot. Its total weight is about 130 [kg] and its height is about 180 [cm]. The mechanism of the low limbs is composed of screw-nuts and connecting rods which are different from the traditional mechanism of the humanoid robot, such as harmonic gear and timing belt. The advantage of this mechanism is that it can provide a variable transmission ratio which can be used to reduce the motor power during walking. Fig. 2 shows the transmission part of ankle joint.

The actuators of the low limbs were selected by the simulation of several specific walking patterns in the sagittal and lateral plane. Contrary to the lower limbs, the design objective of the upper body was more focused on the lightweight and compact structure rather than the power analysis.

### B. Control System Hardware Architecture

The control system of THBIP-I is a parallel multi-computer architecture and can be divided into the following subsystems: *remote brain work station* (RBW), *mobile controller* (MC), *distributed control units* (DCU), and *sensor processing unit* (SPU) [9].

The RBW subsystem is responsible for path planning and some actions that cannot be operated by the autonomous robot body. The MC subsystem is a laptop computer embedded in the body of the robot, and it can collect environmental information by sensors and generate the compensate trajectories from pre-recorded joint trajectories. RBW and MC are connected by a wireless Ethernet. DCU is divided into two parts: high level control and low level control. High level is composed by two PC-104 embedded computers responsible for upper limbs and lower limbs respectively. Low level is composed by 11 PID servo control units. Each servo control unit is made up of two CPU computer systems and mounted on the limbs to control nearly three and four joints. Each joint of the robot is actuated by Maxon electronic brushless DC motor. The PC-104 and servo control units are connected by

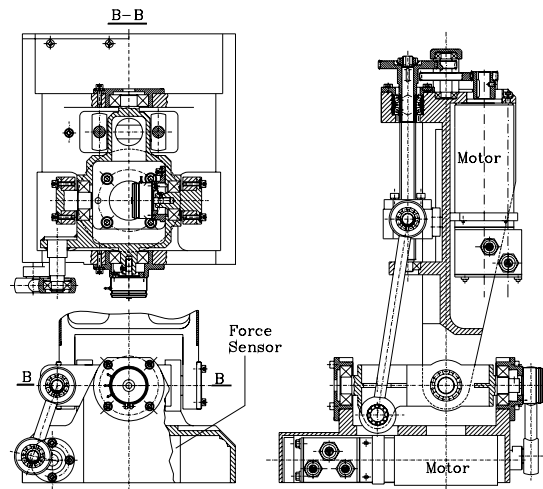


Fig. 2 Mechanism of the 2 DOF ankle joints

CAN bus and two PC-104 systems are connected to MC with Ethernet. SPU is another PC-104 computer, which deals with the data processing of a gyrometer, an accelerometer, and two 6-axis force/torque sensors. Besides these four subsystems, an energy management regulates the power supply from battery to control system and motors.

### C. Sensors in the robot

Two 6-axis force/torque sensors are placed in the feet to measure the ground reaction force and are used to calculate ZMP position. A gyrometer and accelerometer are mounted in the trunk of the robot to measure the posture and body position of the robot. Two CCD cameras are planted in the head to perceive the environment. These sensors are used to realize feedback control, and they are necessary for stable walking on uneven ground.

## III. GAIT PLANNING ALGORITHM

### A. ZMP Criterion

Compared with industrial manipulators, the interaction between a walking robot and the ground is more complex. The concept of a zero-moment point (ZMP) has been shown to be useful in biped locomotion. The ZMP represents the point at which the ground reaction force is taken to occur. Using the ZMP we can synthesize the walking patterns of biped robots and demonstrate a walking motion with actual robots. Thus, the ZMP criterion dictates the dynamic stability of a biped robot. The location of ZMP can be calculated using a model of the robot. If the ZMP is within the convex hull of all contact points (the stable region), the biped humanoid robot is possible to walk.

### B. Trajectories Generation Based on Optimization of the Main Support Leg

This section brings forward a walking gait planning algorithm based on optimization of the main support leg. The gait cycle is generated in deep optimizations.

*Main Support Leg* is defined as the leg in which the foot has a fully contact with the ground. The kinetic properties of the main support leg will mainly determine the stability of the

robot [10].

As shown in Fig. 3, we define five key postures from left to right as:  $\{\theta_i\}_{DblSpprt}$ ,  $\{\theta_i\}_{LvngGrnd}$ ,  $\{\theta_i\}_{CntrGrnd}$ ,  $\{\theta_i\}_{SwngGrnd}$ , and  $\{\theta_i\}_{DblSpprt}^{sym}$ . The fifth posture is the symmetry posture of the first one.

During the whole gait cycle, there are two parts of double support phases and a single support phase. Between  $\{\theta_i\}_{DblSpprt}$  and  $\{\theta_i\}_{LvngGrnd}$ , and between  $\{\theta_i\}_{SwngGrnd}$  and  $\{\theta_i\}_{DblSpprt}^{sym}$ , there are two parts of double support phase, and we call these two part double support phases “heel-off double support phase”, and “toe-off double support phase” separately. Between  $\{\theta_i\}_{LvngGrnd}$  and  $\{\theta_i\}_{SwngGrnd}$ , there is a single support phase. For convenience and clarity in this paper, we call it “back-lean single support phase” between  $\{\theta_i\}_{LvngGrnd}$  and  $\{\theta_i\}_{CntrGrnd}$ , while we call it “forward-lean single support phase” between  $\{\theta_i\}_{CntrGrnd}$  and  $\{\theta_i\}_{SwngGrnd}$ .

We first determine the posture  $\{\theta_i\}_{DblSpprt}$  in which two soles of the robot both contact with the ground completely. This posture is determined by an optimization process. The target of the optimization is to minimize the sum of the angles differences between the two postures  $\{\theta_i\}_{DblSpprt}$  and  $\{\theta_i\}_{DblSpprt}^{sym}$ . When the optimization terminates, such postures ensure that the status of the main support leg change least and the potential of stability in a certain extent.

Secondly, we need to determine the time intervals. According to the human gait, we predetermine a time variable  $T_{cof}$ , and we can attain the following time intervals

$$\text{Heel-off double support phase:} \\ T_1 = T_{cof} \cdot StepDuration \quad (1)$$

$$\text{Backward-lean single support phase:} \\ T_2 = (0.5 - T_{cof}) \cdot StepDuration \quad (2)$$

$$\text{Forward-lean single support phase:} \\ T_3 = (0.5 - T_{cof}) \cdot StepDuration \quad (3)$$

$$\text{Toe-off double support phase:} \\ T_4 = T_{cof} \cdot StepDuration \quad (4)$$

In our research, when  $T_{cof}$  varies from 0.23 [s] and 0.26 [s], practical dynamic gaits differ from each other very little;

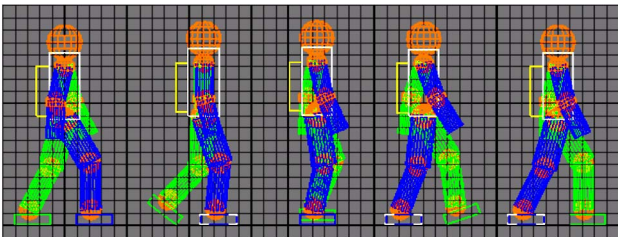


Fig. 3 Key postures in the gait cycle

therefore, we specify  $T_{cof} = 0.25$  [s] particularly.

After the posture  $\{\theta_i\}_{DblSpprt}$  and the time intervals are determined, we still need to determine the states of the main support leg. We use three parameters  $\alpha_{ankle}^U$ ,  $\alpha_{knee}^U$ , and  $\gamma_{del}$  to parameterize the states of the main support leg. The meaning of the four parameters can be found in [10]. Fig. 4 shows the whole process that generates the dynamic gait cycle.

#### IV. CONTROL STRATEGY

##### A. Overall Control Strategy

In order to stable walking, local joint controller and online sensor feedback controller are needed [11].

A new compound joint controller is presented to accomplish biped locomotion for THBIP-I. This controller consists of feed-back control, feed-forward compensation, and mechanical resonance suppressing. It can greatly enhance the gait-tracking ability and suppress the mechanical resonance. This method is also suitable for other humanoid robots, especially those with low mechanical inherent frequency.

Three online sensory feedback controllers were implemented: torso posture controller, ZMP fuzzy compensator, and Impact Reducer. Fig. 5 shows the overall block diagram for dynamic walking control.

##### B. Local Joint Controller

The joint control is a fundamental problem to humanoid robot. With a traditional PID controller, it is difficult to solve the following problems at the same time: the nonlinear transmission mechanism, the coupling effect among joints, and the low inherece frequency. Moreover, it can not solve the mechanical resonance problem which is caused by the low

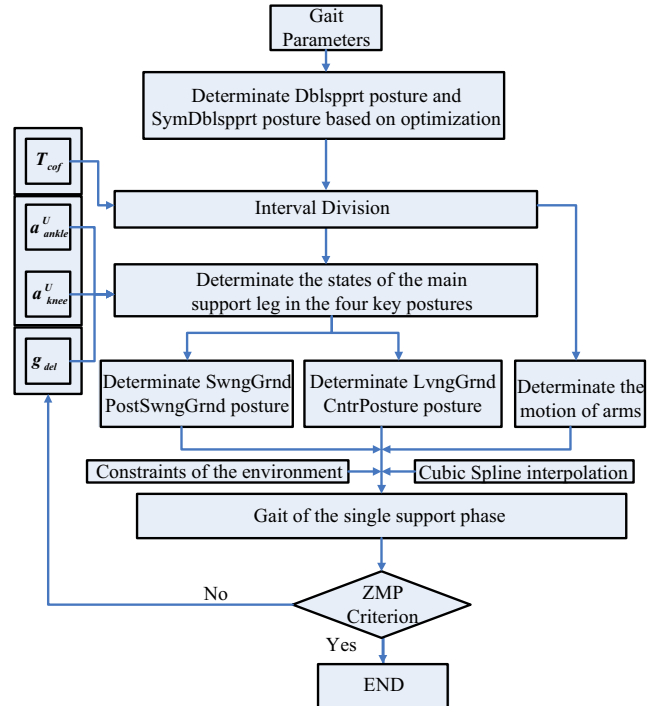


Fig. 4 Flow chart of planning fast dynamic walking gait

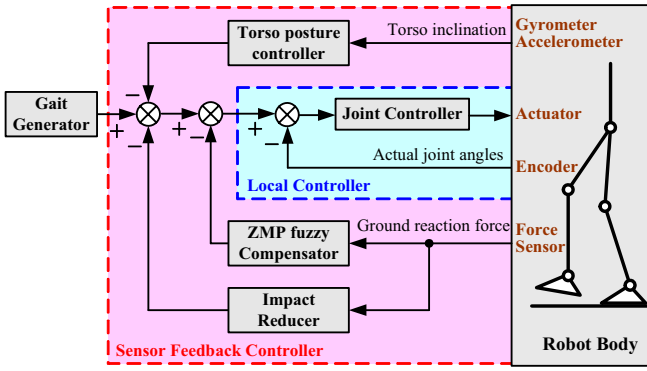


Fig. 5 Overall control strategy for dynamic walking

stiffness and damp of the mechanical parts.

To get a precise model of each joint, we do some identification experiments. A certain frequency sine signal is inputted into the system and the same frequency angle signal can be measured by the potentiometer. Comparing the change of magnitude and phase on the different frequency point, we can get the approximate transfer function of each joint.

Although we adopt nonlinear transmission part, we assume that each joint axis is regarded as a linear single-input/single-output system with the nonlinear dynamic coupling effects treated as disturbances. This is reasonable, because the dynamic coupling and nonlinear transmission acting on the actuator axis among the links are reduced largely by the reducer of high ratios and then suppressed by the error driven control law. Therefore, the joint controller is designed with the typical goal of achieving good disturbance rejection and trajectory tracking ability.

Usually, the transfer function of DC motor position servo system can be simply expressed as:

$$G(s) = \frac{K_p}{s(T_e s + 1)(T_m s + 1)} \quad (5)$$

Comparing with frequency responding data of each joint, the parameters  $K_p$ ,  $T_e$ , and  $T_m$  can be obtained by minimum mean-square method.

To enhance the gait-tracking ability, we adopt compound controller composed of feed-back PID controller and feed-forward compensation. Detailed process knowledge is required for the design of a feed-forward controller. This is a prior knowledge obtained by the previous identification.

With the above controller we presented, the robot can walk under such a gait: step length of 300 [mm], and step duration of 6 [sec]. Gait tracking error of each joint is limited below 0.5 [deg], Section V will show the experimental results.

However, another problem is the vibration of the ankle joint during walking, and this is caused by the low stiffness and the large clearance between mechanical transmission parts. From the two 6-axis force sensors, we can know that the resonance frequency is about 1.5 Hz.

As shown in Fig. 6, we established a simple model of ankle joint based on linear inverted pendulum. We assume that the vibrating model can be simplified as an inverted pendulum,

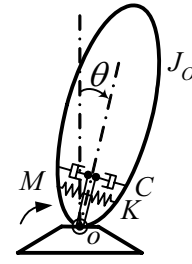


Fig.6 Model of the ankle joint

and the ankle joint can be linearized as a spring-damper system. Its dynamics equation can be expressed approximately as

$$J \cdot \ddot{\theta}(t) + C \cdot \dot{\theta}(t) + K \cdot \theta(t) = M(t) \quad (6)$$

Its Lagrange transformation can be derived as,

$$J s^2 \cdot \theta(s) + C s \cdot \theta(s) + K \cdot \theta(s) = M(s) \quad (7)$$

$$\begin{aligned} \frac{\theta(s)}{M(s)} &= \frac{1}{J s^2 + C s + K} \\ &= \frac{1/K}{\frac{J s^2}{K} + \frac{C}{K} s + 1} = \frac{1/K}{\frac{s^2}{\omega_r^2} + 2\zeta \frac{s}{\omega_r} + 1} \end{aligned} \quad (8)$$

$$\text{where } \omega_r = \sqrt{\frac{K}{J}}, \quad \zeta = \frac{C}{2\sqrt{K \cdot J}}.$$

The new transfer function of position servo system can be derived as:

$$G(s) = \frac{Kp}{s(T_m s + 1)(T_e s + 1) \left( \frac{s^2}{\omega_r^2} + 2\zeta \frac{s}{\omega_r} + 1 \right)} \quad (9)$$

To reduce this vibration, we add the following controller to the feed-back channel:

$$\frac{\frac{s^2}{\omega_r^2} + 2\zeta \frac{s}{\omega_r} + 1}{(T_1 s + 1)(T_2 s + 1)} \quad (10)$$

where  $\zeta \ll 1$ ,  $T_1 \gg T_2$ ,  $\omega_r = 1.5\text{Hz}$

A pair of conjugate poles which cause resonance can be eliminated through this controller, so the system transfer can be expressed as following:

$$G(s) = \frac{K}{s(T_m s + 1)(T_e s + 1)(T_1 s + 1)(T_2 s + 1)} \quad (11)$$

Fig.7 shows the diagram of the joint controller.

### C. Sensory Feedback Controller

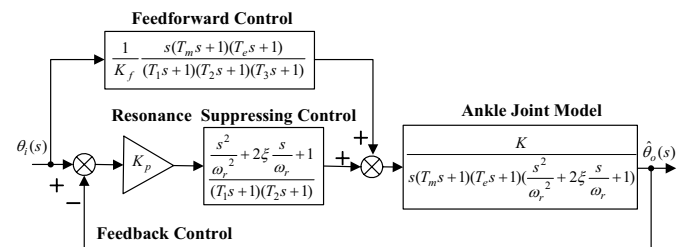


Fig. 7 The diagram of ankle joint controller

Three online sensor feedback controllers were implemented: torso posture controller, ZMP fuzzy compensator, and Impact Reducer, as shown in Fig. 7. Torso posture controller is used to maintain the desired torso posture, since a biped robot tends to tip forwards/backwards if its torso leans forwards/backwards. Since the hip joints are near the torso, the most effective way to maintain the desired torso posture is to control the hip joints [11]. ZMP fuzzy compensator is used to make the actual ZMP coincide with the desired ZMP as near as possible [12]. Since the support ankle joint has the largest effect on ZMP, the most effective way to compensate ZMP is to control the support ankle joint. Impact Reducer is used to reduce the impact force when the swing foot touches ground.

Considering the length of this paper, we only introduce the ZMP fuzzy compensating Controller (ZCC).

As shown in Fig. 8, the control process of ZCC is summarized as follows: (1) Calculate the position error of the ankle joint ( $e_i = \theta_{d,i} - \theta_{a,i}$ ), and the ZMP error ( $\Delta zmp = zmp_a - zmp_d$ ), where  $\theta_{d,i}$  is the desired joint position,  $\theta_{a,i}$  is the actual joint position,  $zmp_d$  is desired ZMP,  $zmp_a$  is the actual ZMP. (2) Use  $\Delta zmp$  and the change of  $\Delta zmp$  as two input variables of a self regulating fuzzy controller, and infer the compensation angle  $\theta_{r,i}$  of the pitch and roll joint of the support leg. (3) Compute the regulated joint position  $\theta_{t,i} = e_i + \theta_{r,i}$  and input this value to joint controller.

The structure of self regulating fuzzy controller is shown in Fig. 9, which selects  $\Delta X_{zmp}$  and the change of ZMP error ( $\Delta \alpha X_{zmp}$ ) as two input variables, and the compensation angle as output variable. Considering the magnitude of these two variables and the influence of DOF's rotation direction on actual ZMP, the fuzzy control rules can be formulated as

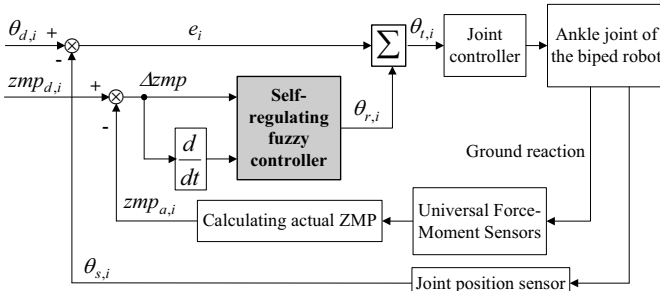


Fig. 8 ZMP fuzzy compensating controller (ZCC) of ankle joint based on ZMP error

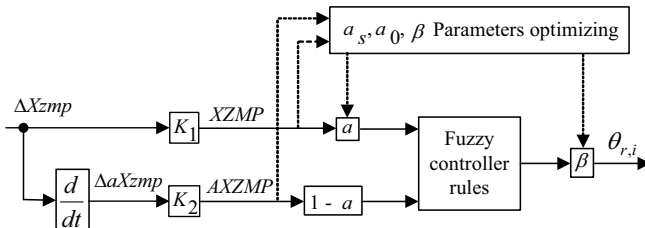


Fig. 9 Self-regulating fuzzy controller

follows:

$$\theta_{r,i} = [\alpha \cdot XZMP + (1 - \alpha) \cdot AXZMP] \cdot \beta \quad (12)$$

$$\alpha = (\alpha_s - \alpha_0) \cdot |XZMP| / N + \alpha_0 \quad (13)$$

where  $0 \leq \alpha_0 \leq \alpha_s \leq 1$ ,  $\alpha \in (\alpha_0, \alpha_s)$ .

Based on the ITAE rule, the values of weighted factor  $\alpha$  and  $\beta$  are self-optimized by minimizing the cost function:

$$\Delta Q = t \cdot |\Delta X_{zmp}| \cdot \Delta T \quad (14)$$

where  $\Delta T$  is the sampling interval which is 20 ms particularly in THBIP-I, and  $t$  is the runtime of the controller.

## V. EXPERIMENTAL RESULTS

In this section, we utilize the above planing method and control strategy to discuss the stable biped locomotion experiments.

With the controller we presented above, the robot can walk stably and smoothly under such a gait: step length of 300 mm, and step duration of 6 seconds.

Fig.10 shows the comparison of planning and real position trajectories of ankle joint when the robot walks. The 4 DOF from bottom to top are ankle yaw and pitch of both legs. The tracking error is under 0.5 degree.

Fig.11 shows the comparison of moment on the left foot with or without the resonance suppressing controller.

We also did the experiments to evaluate the ZCC controller when the humanoid robot THBIP-I walked with the stride of 30 [cm] and the speed of 10 [s/step]. The basic universes of ZMP error, the change of ZMP error, and the compensation angle correspond to  $(-x_{ze}, x_{ze}) = (-3.0, 3.0)$  mm,  $(-x_{sc}, x_{sc}) = (-0.3, 0.3)$  mm, and  $(-\theta_r, \theta_r) = (-0.1, 0.1)$  degree, respectively. The universe grades of three fuzzy variables are all defined as  $XZMP = AXZMP = IR = \{-6, -5, -4, -3, -2, -1, 0, 1, 2, 3, 4, 5, 6\}$ , and so  $N=6$ ,  $K_1=2$ ,  $K_2=20$ . In addition, the parameters are optimized as follows:  $\alpha_s = 0.90$ ,  $\alpha_0 = 0.76$ ,  $\beta$  of roll and pitch DOF of left ankle  $= (0.02, 0.05)$ , and that of right ankle DOF  $= (0.02, 0.01)$ .

The error of actual ZMP with ZCC controller is much smaller than that of common controller. For example, during the right leg support phase the error of XZMP decreases from  $(-1.8 \sim 5.2)$  to  $(-1.4 \sim 3.0)$ , and the error of YZMP decreases

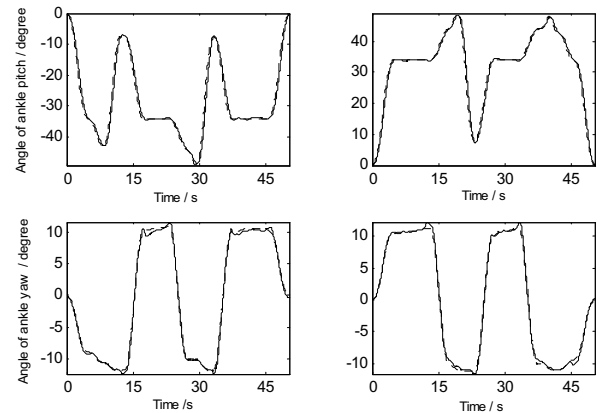


Fig. 10 Planning and Real Trajectories of ankle joint

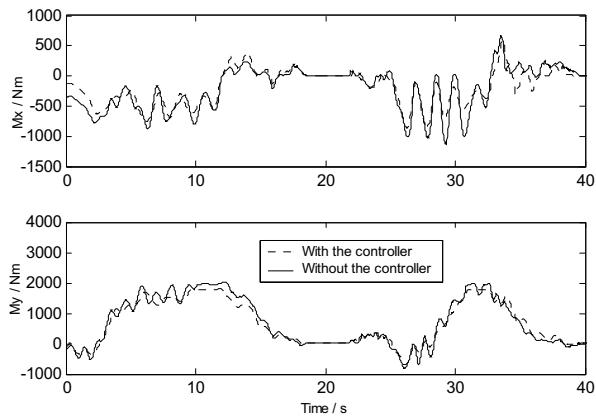


Fig. 11 Comparison of moment of left foot with and without the resonance suppressing controller from (-2.35 ~ 1.85) to (-1.2 ~ 0.2).

Fig. 12 shows the snapshot of walking on flat ground, and Fig. 13 shows the snapshot of climbing up and down stairs.

## VI. CONCLUSION

In this paper, we have studied planning method and control strategy for stable biped walking, and show their realization in THBIP-I humanoid robot. The results of this paper are summarized as follows:

- 1) A 32-DOF humanoid robot platform called “THBIP-I” has been developed. The design issues including mechanical design and control architecture were introduced.
- 2) Gait planning method based on optimization of the main support leg was presented. The gait cycle is generated in deep optimizations.
- 3) Control strategy which combines local joint control and sensor feedback control was prescribed. The local controller was designed to enhance the gait-tracking ability and suppress the mechanical resonance simultaneously. The sensor feedback controller was composed of torso posture controller, ZMP fuzzy compensator, and Impact Reducer. Several experiments were performed to verify the performance of THBIP-I with the proposed control strategy.



Fig.12 Walking on flat ground (Sequence photographs: 2.0 [sec/frame])



Fig.13 Climbing up and down stairs (Sequence photographs: 20 [sec/frame])

## ACKNOWLEDGMENT

The authors would like to thank all the researchers of this project for their collaboration.

## REFERENCES

- [1] Y. Ogura, T. Kataoka, H. Aikawa, K. Shimomura, H. Lim, and A. Takanishi, “Evaluation of Various Walking Patterns of Biped Humanoid Robot,” in *Proc. of the 2005 IEEE Int. Conf. Robotics and Automation*, pp. 605-610, 2005.
- [2] K. Hirai, M. Hirose, Y. Haikawa, and T. Takenaka, “The development of Honda humanoid robot” in *Proc. of the 1998 IEEE Int. Conf. Robotics and Automation*, pp. 1321-1326, 1998.
- [3] K. Nishiwaki, T. Sugihara, S. Kagami, M. Inaba, and H. Inoue, “Realtime generation of humanoid walking trajectory by mixture and connection of pre-designed motions – online control by footprint specification” in *Proc. of the 2001 IEEE Int. Conf. Robotics and Automation*, pp. 4110-4115, 2001.
- [4] S. Lohmeier, K. Löffler, M. Gienger, H. Ulbrich, and F. Pfeiffer, “Computer system and control of biped “Johnnie,”” in *Proc. of the 2004 IEEE Int. Conf. Robotics and Automation*, pp. 4222-4227, 2004.
- [5] Y. Kuroki, M. Fujita, T. Ishida, K. Nagasaka, and J. Yamaguchi, “A small biped entertainment robot exploring attractive applications” in *Proc. of the 2003 IEEE Int. Conf. Robotics and Automation*, pp. 471-476, 2003.
- [6] K. Kaneko, F. Kanehiro, S. Kajita, H. Hirikawa, T. Kawasaki, M. Hirata, K. Akachi, and T. Isozumi, “Humanoid robot HRP-2,” in *Proc. of the 2004 IEEE Int. Conf. Robotics and Automation*, pp. 1083-1090, 2004.
- [7] Q. Huang, Z. Q. Peng, W. M. Zhang, L. G. Zhang, and K. J. Li, “Design of humanoid complicated dynamic motion based on human motion capture,” in *Proc. of the 2005 IEEE/RSJ Int. Conf. Intelligent Robots and Systems*, pp. 3536-3541, 2005.
- [8] L. Liu, J. S. Wang, K. Chen, J. D. Zhao, and D. C. Yang, “The Biped Humanoid Robot THBIP-I,” in *Proc. of the 2001 Int. workshop on Bio-Robotics and Teleoperation*, pp. 164-167, 2002.
- [9] M. G. Zhao, L. Liu, J. S. Wang, K. Chen, J. D. Zhao, and K. Xu, “Control system design of THBIP-I humanoid robot,” in *Proc. of the 2002 IEEE Int. Conf. Robotics and Automation*, pp. 2253-2258, 2002.
- [10] K. Xu, K. Chen, L. Liu, and D. C. Yang, “Fast walking gait planning algorithm for humanoid robots based on optimization of the main support leg,” *Robot*, vol. 27, no. 3, pp. 203-209, 2005. (in Chinese)
- [11] Q. Huang and Y. Nakamura, “Sensory reflex control for humanoid walking,” *IEEE Trans. Robot.*, vol. 21, no. 5, pp. 977-984, 2005.
- [12] J. D. Zhao, Z. Liu, and C. L. Fu, “Self-regulating fuzzy control of ankle joint of a biped humanoid robot based on ZMP error,” in *the 11<sup>th</sup> Int. Symp. on Artificial Life and Robotics*, pp. 695-698, January, 2006.